*AAPS PharmSciTech, Vol. 16, No. 5, October 2015 (© 2015)*
DOI: 10.1208/s12249-015-0293-1

*Research Article*

# Size Control in the Nanoprecipitation Process of Stable Iodine ($^{127}$I) Using Microchannel Reactor—Optimization by Artificial Neural Networks

**Mohamad Hosein Aghajani,[1] Ali Mahmoud Pashazadeh,[2] Seyed Hossein Mostafavi,[3,4] Shayan Abbasi,[5] Mohammad-Javad Hajibagheri-Fard,[6] Majid Assadi,[2] and Mahdi Aghajani[2,3,7]**

*Received 19 November 2014; accepted 12 January 2015; published online 6 February 2015*

***Abstract.*** In this study, nanosuspension of stable iodine ($^{127}$I) was prepared by nanoprecipitation process in microfluidic devices. Then, size of particles was optimized using artificial neural networks (ANNs) modeling. The size of prepared particles was evaluated by dynamic light scattering. The response surfaces obtained from ANNs model illustrated the determining effect of input variables (solvent and antisolvent flow rate, surfactant concentration, and solvent temperature) on the output variable (nanoparticle size). Comparing the 3D graphs revealed that solvent and antisolvent flow rate had reverse relation with size of nanoparticles. Also, those graphs indicated that the solvent temperature at low values had an indirect relation with size of stable iodine ($^{127}$I) nanoparticles, while at the high values, a direct relation was observed. In addition, it was found that the effect of surfactant concentration on particle size in the nanosuspension of stable iodine ($^{127}$I) was depended on the solvent temperature.

**KEY WORDS:** ANNs; microfluidic; nanoprecipitation; particle size; stable iodine.

## INTRODUCTION

Nanosuspension formulation of stable iodine ($^{127}$I) can have a remarkable advantageous over the usual form of iodine. Stable iodine ($^{127}$I) is one of the main preventive measures used for those people near a nuclear event to lessen absorption of released radioiodine in their thyroid glands. Since, in such cases, there is a competition between stable iodine ($^{127}$I) and radioiodine to be absorbed in the thyroid; therefore, nanosuspension form of the stable iodine ($^{127}$I) may increase uptake rate of stable iodine ($^{127}$I) in comparison to radio iodine, reducing uptake of radio iodine. Various nanosizing techniques have been developed to increase dissolution velocity and solubility of drug through enhancing surface area to volume ratio of the drug particles, e.g., nanosuspension engineering. During the formulation of nanosuspensions, drug particles under 1 μm are distributed in an outer liquid phase and are fixed by stabilizers (1,2). The nanosuspension engineering is a simple procedure which is generically applicable for most of drug molecules (3). Also, in comparison of the conventional formulation systems, it is shown that formulation of nanosuspension is associated with advantages such as increased absorption rate, enhanced dissolution, improved bioavailability (4,5), increased adhesion, high drug loading (6,7), and scale-up capability (8).

Typically, during nanosuspensions process, drug nanocrystals are made in a liquid medium using top-down (i.e., milling by media and high pressure homogenizer) or bottom-up (i.e., precipitation) methods. In the precipitation process, a drug is solved in a solvent to produce the supersaturated solution, then mixed with an antisolvent in order for precipitation of drug molecules and form drug nuclei (nucleation) (9). In microfluidic devices technology, the nucleation procedure is performed in microreactors with internal diameters usually smaller than 1 mm (10). The major advantages of microfluidic channel are high surface area to volume ratio and low Reynolds number which refers to laminar flow patterns (i.e., a liquid flows in parallel layers) (11,12). Therefore, a significant reduction in reagents usage, time of experiments, and costs is observed while reproducible experiments and performance are provided (9,13,14). Furthermore, monodispersed particles are commonly obtained in this method. In the microfluidic nanoprecipitation, at first, a

[1] Faculty of Advanced Medical Technology, Golestan University of Medical Sciences, Gorgan, Iran.
[2] Department of Nanotechnology, The Persian Gulf Nuclear Medicine Research Center, The Persian Gulf Biomedical Sciences Institute, Bushehr University of Medical Sciences, Bushehr, Iran.
[3] Department of Medical Nanotechnology, School of Advanced Technologies in Medicine, Tehran University of Medical Sciences, Tehran, Iran.
[4] Nanotechnology Research Centre, Faculty of Pharmacy, Tehran University of Medical Sciences, Tehran, Iran.
[5] Institute of Biochemistry and Biophysics (IBB), University of Tehran, Tehran, Iran.
[6] Shohadaye Khalije Fars Hospital, Bushehr University of Medical Sciences, Bushehr, Iran.
[7] To whom correspondence should be addressed. (e-mail: m.aghajani@bpums.ac.ir; m_aghajani@razi.tums.ac.ir; mehdinano88@gmail.com)

 

supersaturated solution of drug is prepared by dissolving the drug in a solvent. The solution obtained is then injected into an antisolvent, as a poor solvent, to form and grow of nucleation sites on the fluids interface (see Fig. 1). Using surfactant to limit drug crystal growth, it is possible to prevent creation of microparticles.

Effects of changing the various parameters of the microfluidic precipitation process, including flow rate of drug solution and antisolvent, drug saturation level, channels internal diameter, microreactor inlet angle, drug concentration, precipitation temperature, and surfactant concentration, on the size of nanosized drug particles have been evaluated widely in previous studies (15–20). It is observed that increasing in the flow rate of antisolvent and decreasing in the flow rate of drug solution, sharpen inlet angles and lessen saturation levels resulted in smaller particle sizes (19). In another study, it was shown that design of microreactor and processing conditions may have an influence on the hydrocortisone particle size during nanoprecipitation using microfluidic reactors (18). Also, microfluidic nanoprecipitation of the other pharmaceutical ingredients such as danazol (20), norfloxacin (15), cefuroxime axetil (16), and rifampicin (17) have shown the creation of drug particles with controlled sizes, improved dissolution rate, continuous synthesis, and amorphous profile.

In this study, we used artificial neural networks (ANNs) to find a predictive and quality model describing the effects of experiment parameters (independent variables) on the particle size (dependent variable) of the stable iodine ($^{127}$I) nanosuspension formulation obtained by nanoprecipitation in microfluidic reactors. ANNs are artificial intelligence tools which arbitrary find the nonlinear and complex relation between the experimental data (21). It can be used to predict the relations between independent variables (i.e., inputs) and corresponding dependent variable(s) (i.e., output(s)) (19), especially in case of complex experimental data in nanotechnology studies (22).

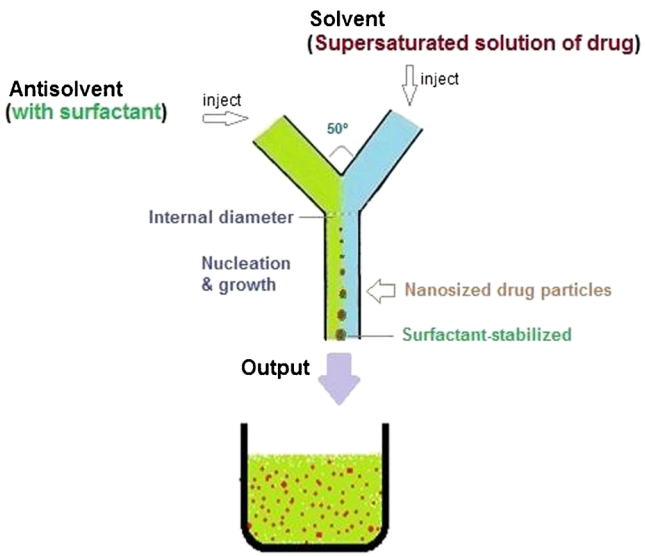


**Fig. 1.** Schematic of nanoprecipitation in microfluidic channels (with the 1 mm internal diameter)

## MATERIALS AND METHODS

### Materials

For the present study, potassium iodide (KI) (Merck chemicals, Germany), Tween 80 (polysorbate 80) (Sigma-Aldrich, USA), and absolute ethyl alcohol (ethanol) 99/6% (*V*/*V*) (Jahan Alkol Teb Arak co. (JATA), Iran) were used as preliminary materials to set experiment up.

### Stable Iodine ($^{127}$I) Nanoprecipitation in Microchannel Reactor

In order to prepare nanosuspension of stable iodine ($^{127}$I) using microfluidic devices, supersaturated solutions of stable iodine ($^{127}$I) in distilled water (as solvent) at given temperatures (24–80°C) were pumped to the microreactor. Certain flow rates of solvent (0.5–2.4 ml/min) and antisolvent (0.5–2.5 ml/min) were controlled using pumps (Fanavaran Nano-Meghyas, Iran). Also, ethanol as antisolvent system was mixed with predetermined concentrations of surfactant (Tween 80) at the controlled lab temperature of 24±2°C. Temperature of solvent solution was predetermined and controlled by heater throughout the study. Microfluidic instrument was fabricated from the Aluminum material, with internal diameter of 1 mm and inlet angle of 50°. In order to prevent particles growth in prepared nanosuspension, the particle size was measured freshly using dynamic light scattering. Experimentally, 45 samples at random values from four independent variables (i.e., input factors) including solvent flow rate (ml/min), solvent temperature (°C), antisolvent flow rate (ml/min), and surfactant concentration (mg/5 ml) were prepared, and size of samples was considered as dependent variable (i.e., output). Obtained data from experimental study were used to achieve a model by ANNs modeling to understand effects of four input factors on the particle size of prepared nanosuspension through nanoprecipitation in microchannel reactor.

### ANNs Modeling

Modeling of the relations between four input factors and one output parameter was studied using commercially available ANNs software (INForm v4.02, Intelligensys, UK). Then, the response surfaces, illustrated as 3D-graphs, were applied to evaluate the effect of two input parameters on the output parameter while two other input parameters were fixed at given values (i.e., low, medium, and high values).

The results of experimental samples were used to train a model by ANNs. Number of 32 data sets was defined as training data for teaching the network of relations between input variables and output variable. Also, three data set (10% of the training data) were taken as the test data in order to prevent overtraining during the training process. Details of the training parameters (listed in Table I) during the modeling by ANNs have been described previously (23). Following the training of network, ten more data set (as validation data set or unseen data) was also used to evaluate the predictive capability of the model provided by ANNs software. The predictive capability of the obtained model was finally

**Table I.** The Training Parameters Applied in INForm v4.02

| | | |
|---|---|---|
| Network structure | No. of hidden layers | 1 |
| | No. of nodes in hidden layer | 4 |
| Backpropagation type | | Incremental |
| Backpropagation parameters | Momentum factor | 0.8 |
| | Learning rate | 0.7 |
| Targets | Maximum iterations | 1000 |
| | MS error | 0.0001 |
| | Random seed | 10,000 |
| Smart stop | Minimum iterations | 20 |
| | Test error weighting | 0.1 |
| | Iteration overshoot | 200 |
| | Auto weight | On |
| | Smart stop enabled | On |
| Transfer function | Output | Symmetric sigmoid |
| | Hidden layer | Symmetric sigmoid |

validated using correlation coefficient ($R^2$) close to one (24) calculated for unseen data set (see Table II).

### Particle Size Measurement

Relying on the impact of input parameters on the output parameter predicted by obtained model, an optimum formulation (i.e., nanosuspension of stable iodine ($^{127}$I) with minimum size) was prepared and evaluated to determine particle size and morphology.

### DLS Analysis

Particle size (statistical mean value of particle diameter) in optimum formulation was measured by dynamic light scattering (Nano ZS, Malvern instruments, UK) with PCS software (version 1.27). All samples were analyzed at lab temperature (controlled at 22°C), freshly diluted by adding 2 ml deionized water to 1 ml of sample.

### TEM Analysis

Evaluating of the nanoparticle size and its morphology of stable iodine ($^{127}$I) in the optimized nanosuspension formulation was implemented using transmission electronic microscope (Zeiss EM 10C, Germany).

The optimized sample was dispersed in deionized water by ultrasonic for 3 min. Two drops of the nanosuspension sample were put on the copper grid coated by carbon and placed in lab temperature for 15 min (drying sample). Subsequently, the grid was put on a holder to be monitored using TEM at the voltage of 80 kV.

### Determination of Stability

Optimization of the stability of the nanosuspension formulation of stable iodine (127I) demands another study that was out of the scope of our study. Here, physical stability of obtained nanosuspension formulation of stable iodine (127I) with minimum size was investigated, in which time of sedimentation was considered as indicator of physical stability of nanosuspension. Obtained formulation (i.e., sample with minimum particle size) was observed daily, in controlled lab temperature of 24±2°C, in order to determine the time of phase separation of nanoparticles in nanosuspension.

### Determination of Entrapment Efficiency of Stable Iodine ($^{127}$I)

The percentage of entrapment efficiency was measured using spectrophotometric detection at 226 nm. At first, nanosuspension sample of stable iodine obtained (i.e., sample with minimum particle size) was centrifuged at speed of 10,000 rpm for 20 min, at temperature of 20°C. Then, supernatant was separated and content of the free dissolved stable iodine (127I) was detected by UV–vis spectrophotometer at 226 nm. The amount of nanosized stable iodine ($^{127}$I) was determined by subtraction of amount of initial stable iodine ($^{127}$I) minus the free stable iodine ($^{127}$I) (25). This amount can be entrapment efficiency (EE %) according to the following equation:

$$\text{Entrapment efficiency (EE\%)} = \frac{\text{initial drug amount} - \text{free drug amount}}{\text{initial drug amount}} \times 100$$

## RESULTS

After the model was generated by ANNs, $R^2$ values of 0.92, 0.81, and 0.80 were obtained for training, test, and

**Table II.** The Unseen Data Sets Used by ANNs Software

| Solvent flow rate (ml/min) | Solvent temperature (°C) | Antisolvent flow rate (ml/min) | Surfactant concentration (mg/5 ml) | Observed particle size (nm) | Predicated particle size (nm) |
|---|---|---|---|---|---|
| 1.0 | 80 | 1.0 | 1296 | 185.4 | 199.3 |
| 1.8 | 60 | 0.8 | 1296 | 104.0 | 117.1 |
| 2.0 | 60 | 1.0 | 864 | 109.0 | 116.7 |
| 0.8 | 60 | 2.5 | 1296 | 105.0 | 104.9 |
| 2.0 | 40 | 0.5 | 1080 | 169.0 | 175.1 |
| 1.0 | 70 | 2.5 | 1296 | 102.2 | 124.7 |
| 2.0 | 60 | 2.1 | 1252.8 | 52.1 | 60.4 |
| 1.8 | 70 | 1.8 | 972 | 116.0 | 129.4 |
| 1.0 | 50 | 1.0 | 1252.8 | 125.8 | 128.4 |

unseen data, respectively. Resulted values show a satisfactory trained model. Subsequently, the generated model was used to evaluate the effect of above-mentioned input parameters on the particle size in nanosuspension formulation of stable iodine ($^{127}$I). The first choice to determine the relations of input variables and output parameter could be the method of sensitivity analyses. In the current study, an alternative systematic method reported previously (26) was used to determine relations between the input variables and output. As described previously (19), in this method, the effect of changes in two input variables on output parameter (i.e., the particle size) is shown by response surfaces, whereas the remaining input variables are fixed on the predetermined low, mid-range, and high amounts.

Considering the procedure explained above, at first, in order to study change of particle size of stable iodine ($^{127}$I) nanosuspension against solvent and antisolvent flow rate, the other two input variables were fixed at the low, mid-range, and high values, namely, 936.0, 1024.0, and 1290.0 mg/5 ml for Tween 80 concentration and 42, 60, and 78°C for solvent temperature. Resulted three-dimensional graphs are displayed in Fig. 2. According to these graphs, the effect of antisolvent flow rate on nanoparticles size, for every fixed data set, clearly shows that an increase in antisolvent flow rate has led to a considerable decrease in the particle size of stable iodine ($^{127}$I) nanosuspension. Also, it is obviously demonstrated that particles size in the formulation of generated nanosuspension has decreased when the solvent flow rate in nanoprecipitation process has increased.

Figure 3 shows the effect of Tween 80 concentration and solvent flow rate on the particle size of stable iodine ($^{127}$I) nanosuspension in creation of 3D graphs, when other two variables, antisolvent flow rate and solvent temperature, are fixed at the values of low, mid-range, and high (i.e., 0.9, 1.7, and 2.3 ml/min for antisolvent flow rate, and 42, 60, and 78°C for solvent temperature).

It is clear that increasing Tween 80 concentration in the low and mid-range data set of fixed solvent temperature may lead to reduction in the size of stable iodine ($^{127}$I) nanoparticles in nanosuspension. Nevertheless, for the higher values of fixed solvent temperature, an increase in the nanoparticles size after rising Tween 80 concentration is obvious. Also, it is

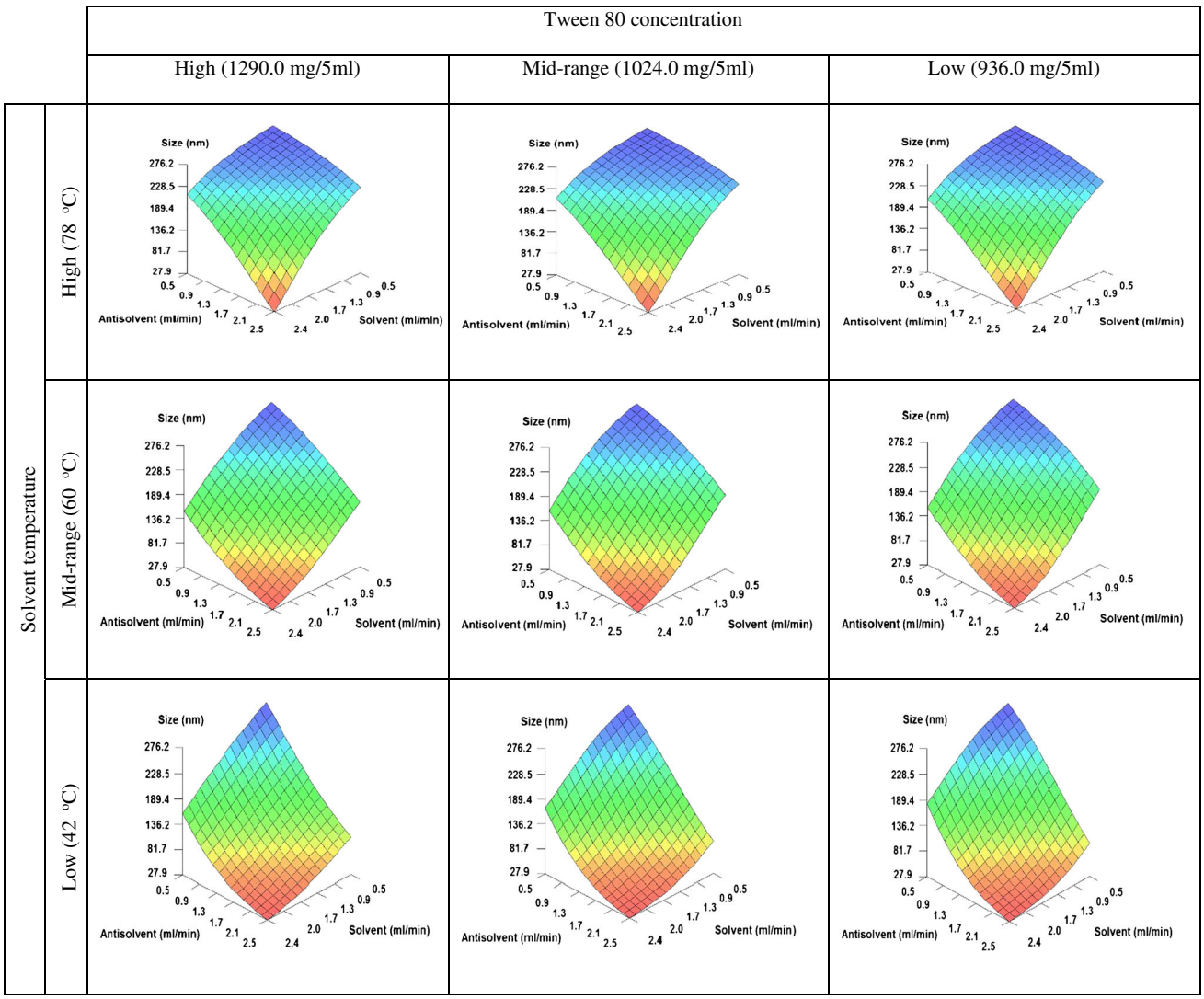


**Fig. 2.** 3D plots of the nanosuspensions size predicted by the ANNs model fixed at low, mid-range, and high values of the Tween 80 concentration and solvent temperature

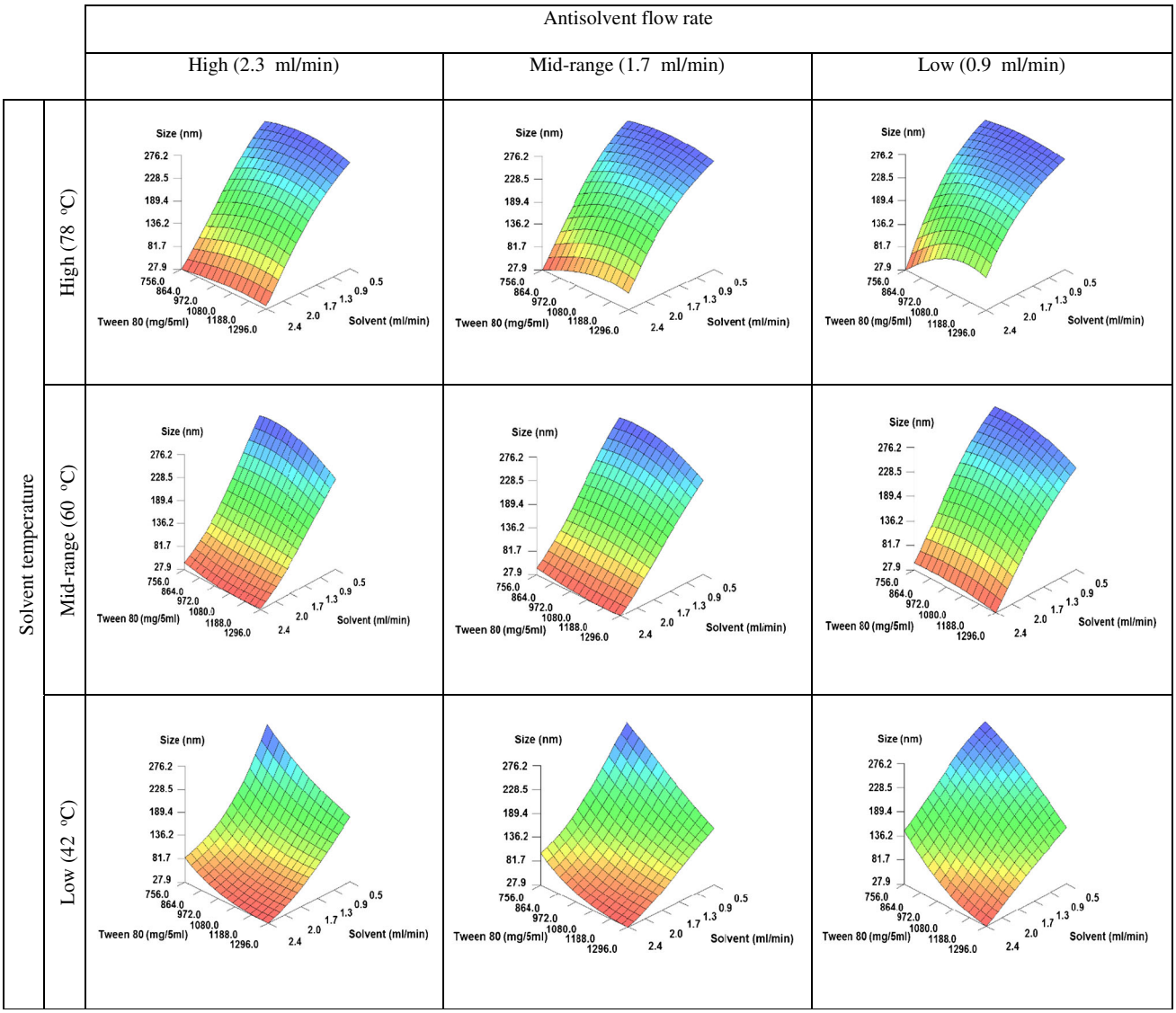


**Fig. 3.** 3D plots of nanosuspensions size predicted by the ANNs model fixed at low, mid-range, and high values of the antisolvent flow rate and solvent temperature

shown that for each data set of fixed antisolvent flow rate and solvent temperature, any increase in solvent flow rate may lead to a considerable reduction in the particle size of obtained nanosuspension, as mentioned above.

Obtained 3D graphs in Fig. 4 show the effect of changes in solvent temperature and Tween 80 concentration on the particles size, when solvent flow rate and antisolvent flow rate are fixed in the amount of low, mid-range, and high (0.9, 1.7, and 2.3 ml/min for both data set). Based on Fig. 4, at low solvent temperature of ~45°C, the particle size in nanosuspension is minimum, showing an indirect relation with lower temperatures and direct relation with higher solvent temperatures. Information on the rows and columns in Fig. 4 show that for both data sets of fixed antisolvent and solvent flow rate, increasing the concentration of Tween 80 results in small decrease in the nanoparticles size of stable iodine ($^{127}$I).

With attention to the details in Figs. 5, 6, and 7 that show the changes of nanoparticles size against Tween 80 concentration and flow rate of antisolvent, solvent temperature and flow rate of antisolvent, and flow rate of solvent and solvent temperature, respectively, the following findings which is indicated above can be obtained:

I. Increasing flow rate of solvent and antisolvent during the nanoprecipitation process can cause to a considerable reduction in the particle size in nanosuspension.
II. The relation between size of iodine nanoparticles and solvent temperature is direct and indirect for high and low temperatures, respectively.
III. In the low (or mid-range) and high ranges of the solvent temperature, respectively, increasing the Tween 80 concentration results in a decrease and increase poorly at the size of nanoparticles obtained during nanoprecipitation.

Also, in this study, polydispersity index (PDI) of nanosuspension samples was determined in the range of

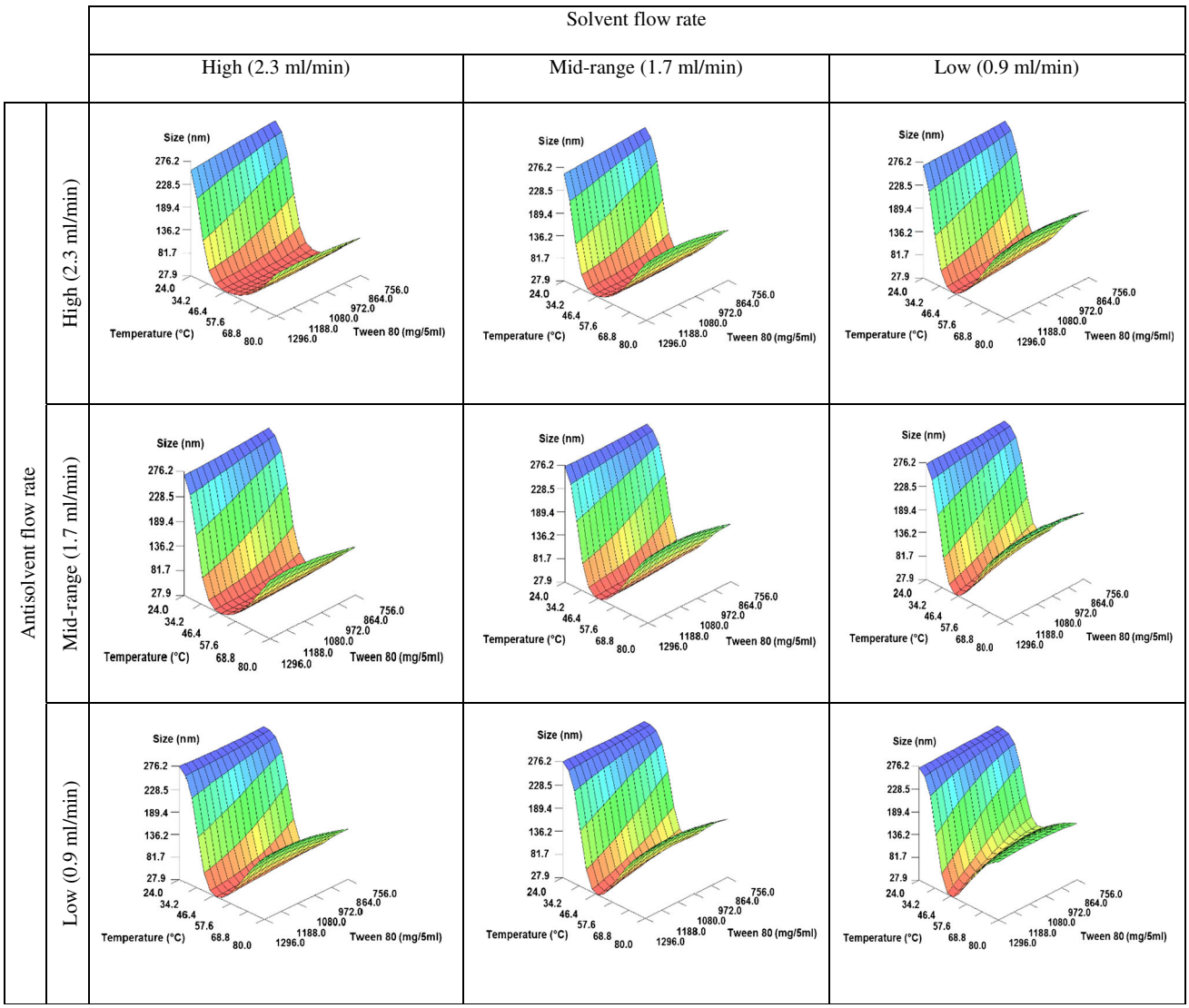


**Fig. 4.** 3D plots of nanosuspensions size predicted by the ANNs model fixed at low, mid-range, and high values of the solvent flow rate and antisolvent flow rate

0.09–0.38, which is normal range obtained in microchannel devices and so their good potential to generate the monodispersed colloidal disperses, as reported in the former works (27,28).

After considering all findings, a new nanosuspension formulation of stable iodine ($^{127}$I) was created to achieve minimum particle size. The nanosuspension sample was prepared in solvent flow rate of 2.4 ml/min, antisolvent flow rate of 2.5 ml/min, solvent temperature of 45°C, and Tween 80 concentration of 1296 mg/5 ml. Particle size of the generated sample was determined ~20 nm which was evaluated by DLS and confirmed using TEM (see Fig. 8).

### Physical Stability of Nanosuspension of Stable Iodine ($^{127}$I)

Sedimentation time of obtained nanosuspension of stable iodine (127I) with minimum particle size was determined by visual observation. Visual observation of sedimentation is one of the methods to estimate stability of prepared nanosuspension (6,9). As nanosuspension of stable iodine is a deflocculated nanosuspension and produced a densely packed sediment, sedimentation can be seen by the visual observation. Finally, physical stability of obtained sample was determined as 68 days.

### Entrapment Efficiency of Stable Iodine ($^{127}$I)

The entrapment efficiency of nanosuspension formulation of stable iodine ($^{127}$I) with minimum particle size was determined to be ~82%. This finding show that almost 82% of supersaturated solution of potassium iodide (KI) powder was converted into stable iodine ($^{127}$I) nanoparticles produced via nanoprecipitation using microfluidic devices.

## DISCUSSION

Up to now, various approaches have been introduced to produce drug nanoparticles. One of the simple and

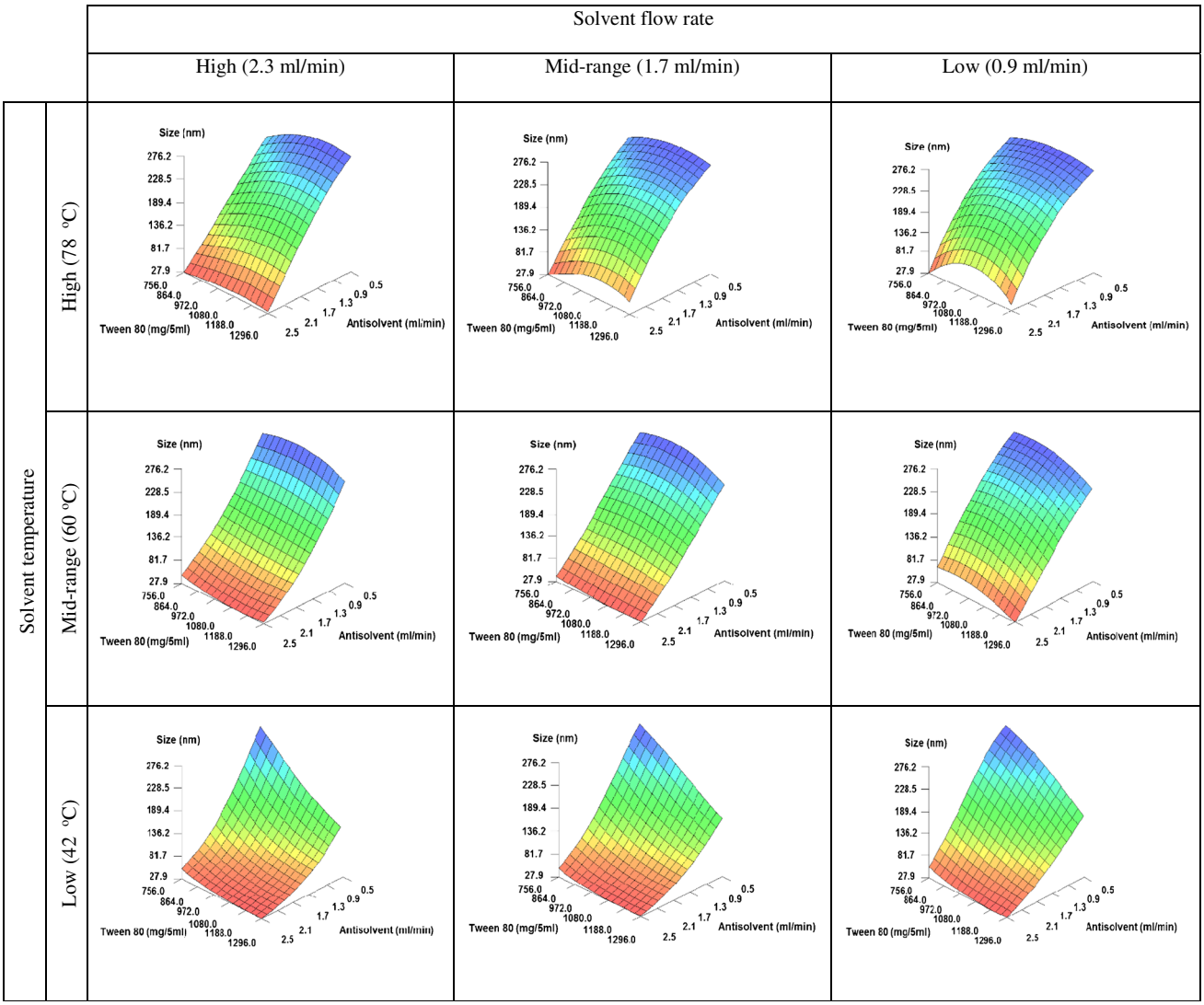


**Fig. 5.** 3D plots of nanosuspensions size predicted by the ANNs model fixed at low, mid-range, and high values of the solvent flow rate and solvent temperature

cost-effective methods to prepare nanoparticles is the use of microfluidics technology (channels with a micrometer scale) (29). It is indicated recently that fluids manipulation and fine control of fluid interfaces in these channels is one of the main benefits of this approach. Controlling the flow and mixing conditions in the microchannels may yield a reproducible monodispersed nanosuspension and provide opportunity to better control of particle size (27,29).

According to the modeling results of our work, particle size of obtained nanosuspension decreased by increasing flow rate of antisolvent, which is in agreement with work of H.S.M. Ali *et al.* (19). This finding is because of the decrease of drug solubility, by adding antisolvent to the solvent (increased mixing), which enhances the level of supersaturation and consequently results in a higher nucleation rate than growth rate. Subsequently, this process leads to generation of smaller nanosized particles (20). Also, any increase in the flow rate of antisolvent can result in diminishing the diffusion process of drug molecules to antisolvent stream per unit volume of antisolvent. This phenomena can cause to fewer solute concentration around growing drug nanocrystal, leading to formation of smaller nanoparticles (19,29).

In addition, by increasing flow rate of solvent in stable iodine ($^{127}I$) nanoprecipitation, the particle size of prepared nanosuspension decreased, which this finding is similar to that of Y.F. Su *et al.* regarding preparation of continuous nanoparticle using microfluidic-based emulsion (30). In fact, this finding may be due to enhancement in the supersaturation level against increased mixing, obtained with increase at flow rate of solvent (18,30). Consequently, increasing nucleation than growth and reduction of particle size can be seen, as expressed above.

From the results mentioned above, the particles size increased in nanosuspension against higher and lower values of solvent temperature, while minimum particle size was observed at low range of solvent temperature near to a certain

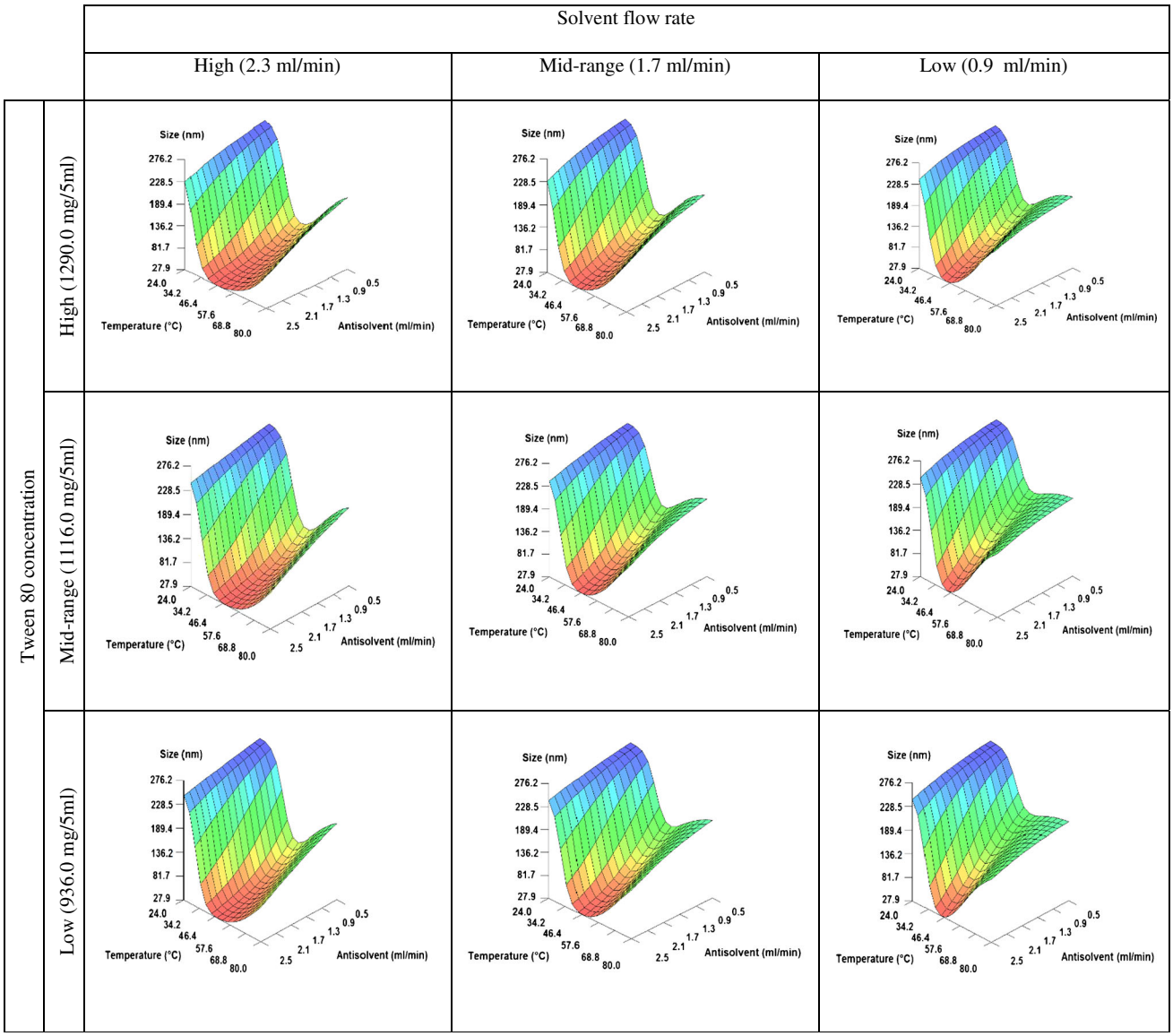


**Fig. 6.** 3D plots of nanosuspensions size predicted by the ANNs model fixed at low, mid-range, and high values of the solvent flow rate and Tween 80 concentration

value (~45°C). It can be argued that the high temperature of solvent leads to increase drug solubility in solvent and consequently, it will be difficult to achieve high supersaturation level during nanoprecipitation process at microfluidic reactor. As a result, this may cause to a low nucleation rate and increased particle size at high temperature values in comparison to low solvent temperature in which solubility of drug in solvent decreases and supersaturation occurs easily (31). Also, nucleation process is a favorable process energetically (i.e., by releasing heat). Therefore, number of created drug nuclei increases at low temperature of solvent (i.e., high nucleation rate/low growth rate and decrease at particle size of output) (32). In addition, with increasing solvent temperature, diffusion of solute molecules into antisolvent flow will increase. So, more drug nuclei will form (i.e., enhanced nucleation than growth) (27) and consequently, particle size in nanosuspension decreases, as observed in lower ranges of solvent temperature (an indirect relation).

The impact of surfactant concentration on particle size is different in low and high values of solvent temperature. The findings in Figs. 3 and 5 show that particle size in nanosuspension decreases against increasing Tween 80 concentration in low (or mid-range) values of solvent temperature, as reported in previous studies by M.E. Matteucci *et al.* and Y. Dong *et al.* (33,34). It is clear that surfactant acts as a steric barrier against particles growth generated by precipitation; as a result, nucleation rate than growth rate increases with enhancing surfactant concentration (33,34). On the other hand, an increase at surfactant concentration in the high values of solvent temperature results in the increasing particle size of output. This may be due to an increase in the diffusion coefficient of surfactant at higher temperature that can result in increasing surfactant molecules uncontrollably on the surface of particles generated during

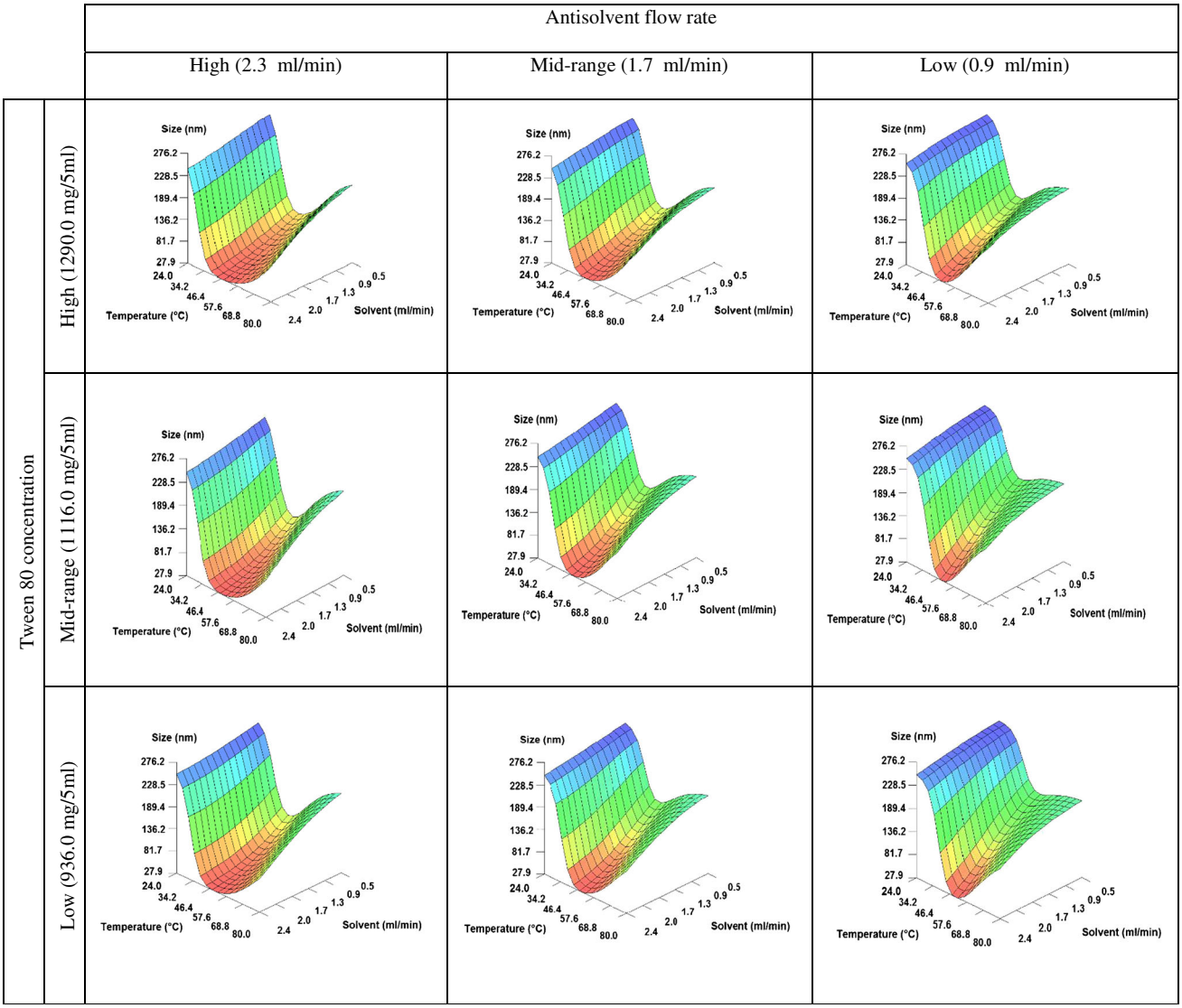


**Fig. 7.** 3D plots of nanosuspensions size predicted by the ANNs model fixed at low, mid-range, and high values of the antisolvent flow rate and Tween 80 concentration

nanoprecipitation at microfluidic channel. Consequently, this can lead to reduce in the mobility of particles dispersed and increase in the observed particle size using dynamic light scattering.

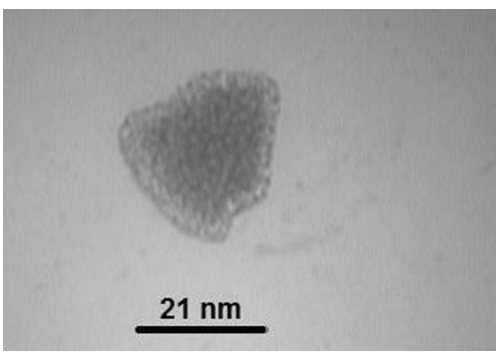


**Fig. 8.** Picture of stable iodine nanoparticle (Transmission Electron Microscope (TEM))

## CONCLUSION

In the current study, modeling by ANNs software has been applied to create a quality model that illustrated effects of solvent flow rate and temperature, antisolvent flow rate, and surfactant concentration on the particle size in nanosuspension formulation of stable iodine ($^{127}$I) obtained by nanoprecipitation technique at microfluidic devices. The obtained response surfaces after modeling showed that input parameters have remarkable impacts on the size of stable iodine ($^{127}$I) nanocrystals. Enhancement of flow rate of solvent and antisolvent caused a decrease in the size of stable iodine ($^{127}$I) nanoparticles. The low and high solvent temperature had an indirect and direct relation, respectively, with particle size of nanosuspension. Also, the size of nanoparticles decreased against increasing the Tween 80 concentration in the low values of solvent temperature, while an increase in Tween 80 concentration at high values of solvent temperature resulted in increasing particle size.

## ACKNOWLEDGMENTS

This project was supported by the vice-chancellor of research at Bushehr University of Medical Sciences and Health Services grant no 20-18-3-46333. The author wishes also to thank Dr. Afshin Ostovar for his support in this research.

**Conflict of Interest** The authors express that they have no conflicts of interest declaration to display.

## REFERENCES

1. Lakshmi P, Kumar GA. Nanosuspension technology: a review. Int J Pharm Sci. 2010;2(4):35–40.
2. Kocbek P, Baumgartner S, Kristl J. Preparation and evaluation of nanosuspensions for enhancing the dissolution of poorly soluble drugs. Int J Pharm. 2006;312(1):179–86.
3. Müller RH, Jacobs C, Kayser O. Nanosuspensions as particulate drug formulations in therapy: rationale for development and what we can expect for the future. Advanced Drug Delivery Reviews. 2001;47(1):3–19.
4. Chingunpituk J. Nanosuspension technology for drug delivery. Walailak J Sci Tech. 2007;4(2):139–53.
5. Lindfors L, Skantze P, Skantze U, Westergren J, Olsson U. Amorphous drug nanosuspensions. 3. Particle dissolution and crystal growth. Langmuir. 2007;23(19):9866–74.
6. Wu L, Zhang J, Watanabe W. Physical and chemical stability of drug nanoparticles. Adv Drug Deliv Rev. 2011;63(6):456–69.
7. Pu X, Sun J, Li M, He Z. Formulation of nanosuspensions as a new approach for the delivery of poorly soluble drugs. Curr Nanosci. 2009;5(4):417–27.
8. Patravale VB, Kulkarni RM. Nanosuspensions: a promising drug delivery strategy. J Pharm Pharmacol. 2004;56(7):827–40.
9. Aghajani M, Shahverdi AR, Rezayat SM, Amini MA, Amani A. Preparation and optimization of acetaminophen nanosuspension through nanoprecipitation using microfluidic devices: an artificial neural networks study. Pharm Dev Technol. 2013;18(3):609–18.
10. Weibel DB, Whitesides GM. Applications of microfluidics in chemical biology. Curr Opin Chem Biol. 2006;10(6):584–91.
11. Voldman J, Gray ML, Schmidt MA. Microfabrication in biology and medicine. Annu Rev Biomed Eng. 1999;1(1):401–25.
12. Crowe CT, Elger DF, Roberson JA. Engineering fluid mechanics. Hoboken: Wiley; 2005.
13. Miyazaki M, Honda T, Yamaguchi H, Briones MPP, Maeda H. Enzymatic processing in microfluidic reactors. Biotechnol Genet Eng Rev. 2008;25(1):405–28.
14. Weigl BH, Bardell RL, Cabrera CR. Lab-on-a-chip for drug development. Adv Drug Deliv Rev. 2003;55(3):349–77.
15. Panagiotou T, Mesite SV, Fisher RJ. Production of norfloxacin nanosuspensions using microfluidics reaction technology through solvent/antisolvent crystallization. Ind Eng Chem Res. 2009;48(4):1761–71.
16. Wang J-X, Zhang Q-X, Zhou Y, Shao L, Chen J-F. Microfluidic synthesis of amorphous cefuroxime axetil nanoparticles with size-dependent and enhanced dissolution rate. Chem Eng J. 2010;162(2):844–51.
17. Schianti JN, Cerize NN, de Oliveira AM, Derenzo S, Seabra AC, Góngora-Rubio MR. Rifampicin nanoprecipitation using flow focusing microfluidic device. J Nanomedicine Nanotechnol. 2013;4(4):2–172.
18. Ali HS, York P, Blagden N. Preparation of hydrocortisone nanosuspension through a bottom-up nanoprecipitation technique using microfluidic reactors. Int J Pharm. 2009;375(1):107–13.
19. Ali HS, Blagden N, York P, Amani A, Brook T. Artificial neural networks modelling the prednisolone nanoprecipitation in microfluidic reactors. Eur J Pharm Sci. 2009;37(3):514–22.
20. Zhao H, Wang J-X, Wang Q-A, Chen J-F, Yun J. Controlled liquid antisolvent precipitation of hydrophobic pharmaceutical nanoparticles in a microchannel reactor. Ind Eng Chem Res. 2007;46(24):8229–35.
21. Agatonovic-Kustrin S, Beresford R. Basic concepts of artificial neural network (ANN) modeling and its application in pharmaceutical research. J Pharm Biomed Anal. 2000;22(5):717–27.
22. Amani A, Mohammadyani D. Artificial neural networks: applications in nanotechnology. Artificial neural networks—application Rijeka. INTECH; 2011.
23. Shao Q, Rowe RC, York P. Comparison of neurofuzzy logic and neural networks in modelling experimental data of an immediate release tablet formulation. Eur J Pharm Sci. 2006;28(5):394–404.
24. Amani A, York P, Chrystyn H, Clark BJ. Factors affecting the stability of nanoemulsions—use of artificial neural networks. Pharm Res. 2010;27(1):37–45.
25. Muthu M, Singh S. Poly (D, L-Lactide) nanosuspensions of risperidone for parenteral delivery: formulation and in-vitro evaluation. Current Drug Deliv. 2009;6(1):62–8.
26. Amani A, York P, Chrystyn H, Clark BJ, Do DQ. Determination of factors controlling the particle size in nanoemulsions using artificial neural networks. Eur J Pharm Sci. 2008;35(1):42–51.
27. Aghajani M, Shahverdi AR, Amani A. The use of artificial neural networks for optimizing Polydispersity Index (PDI) in nanoprecipitation process of acetaminophen in microfluidic devices. AAPS PharmSciTech. 2012;13(4):1293–301.
28. Rosenfeld C, Serra C, Brochon C, Hadziioannou G. Influence of micromixer characteristics on polydispersity index of block copolymers synthesized in continuous flow microreactors. Lab Chip. 2008;8(10):1682–7.
29. Ali HS, York P, Ali A, Blagden N. Hydrocortisone nanosuspensions for ophthalmic delivery: a comparative study between microfluidic nanoprecipitation and wet milling. J Control Release. 2011;149(2):175–81.
30. Su Y-F, Kim H, Kovenklioglu S, Lee W. Continuous nanoparticle production by microfluidic-based emulsion, mixing and crystallization. J Solid State Chem. 2007;180(9):2625–9.
31. Zhang J-Y, Shen Z-G, Zhong J, Hu T-T, Chen J-F, Ma Z-Q, *et al.* Preparation of amorphous cefuroxime axetil nanoparticles by controlled nanoprecipitation method without surfactants. Int J Pharm. 2006;323(1):153–60.
32. Fokin VM, Yuritsyn NS, Zanotto ED. Nucleation and crystallization kinetics in silicate glasses: theory and experiment. Nucleation Theory Appl. 2005:74–125.
33. Matteucci ME, Hotze MA, Johnston KP, Williams RO. Drug nanoparticles by antisolvent precipitation: mixing energy versus surfactant stabilization. Langmuir. 2006;22(21):8951–9.
34. Dong Y, Ng WK, Shen S, Kim S, Tan RB. Preparation and characterization of spironolactone nanoparticles by antisolvent precipitation. Int J Pharm. 2009;375(1):84–8.